First record of an Eomysticetidae from the Late Oligocene at the Pilon locality, San Gregorio Formation, Baja California Sur, Mexico

Cielo Cedillo-Avila, Gerardo González-Barba, and Azucena Solis-Añorve

ABSTRACT

In the paleontological history of cetaceans, the group Chaeomysticeti represents the most basal lineage of baleen whales, as we know them today. Within this group, the family Eomysticetidae, which dates back to the Oligocene Epoch, has been identified in the Northern Hemisphere—specifically in the Pacific Ocean along the coasts of Japan and Mexico, as well as in the Atlantic Ocean in the United States. Additionally, fossils have been discovered in the Southern Hemisphere, particularly in New Zealand. In Baja California Sur, the discovery of Eomysticetidae fossils provides a more comprehensive record than previous findings and enhances our understanding of the relationship between the faunas of the Southern Hemisphere and those of the Northern Hemisphere. So far, one skull, two jaws and the left tympanic bulla have been uncovered, and the level of preservation is conducive to detailing important elements within the family, such as the temporal fossa, the intertemporal region, the length of the nasal bones and the secondary squamosal fossa, among others. Using phylogenetic tools such as TNT software, this anatomic evidence allows us to classify a new genus and species from the Oligocene Epoch.

Cielo Cedillo-Avila. Museo de Historia Natural, Universidad Autónoma de Baja California Sur, Boulevard Forjadores S/N between Street Av. Universidad and Street Félix Agramont Cota Col. Universitario, La Paz, Baja California Sur, 23080 México. cielo.96.cedillo@gmail.com
Gerardo González-Barba. Museo de Historia Natural, Universidad Autónoma de Baja California Sur, Boulevard Forjadores S/N between Street Av. Universidad and Street Félix Agramont Cota Col. Universitario, La Paz, Baja California Sur, 23080 México. gerardo@uabcs.mx
Azucena Solis-Añorve. Museo de Historia Natural and Posgrado of Ciencias Marinas and Costeras (CIMACO), Universidad Autónoma de Baja California Sur, Boulevard Forjadores S/N between Street Av. Universidad and Street Félix Agramont Cota Col. Universitario, La Paz, Baja California Sur, 23080 México. Corresponding author. ca.solis@uabcs.mx

INTRODUCTION

The Oligocene Epoch is considered a time when mysticetes underwent significant diversification (Uhen and Pyenson, 2007; Marx et al., 2016a; Fordyce, 2018; Bisconti et al., 2023). Mysticetes originated in the late Eocene (Priabonian) with the presence of *Mystacodon selenesis* from the Yumaque Formation (Fm.) in Peru (Lambert et al., 2017; de Muizon et al., 2019), and *Llanocetus denticrenatus* from the La Meseta Fm. in Antarctica (Mitchell, 1989; Fordyce and Marx, 2018). The group diversified in the early Oligocene through several lineages of toothed mysticetids, such as Aetiocetidae and Mammalodontidae, which occupied different ecological niches (Barnes et al., 1994; Deméré and Berta, 2008; Tsai and Ando, 2015; Marx et al., 2016b; Geisler et al., 2017; Fordyce and Marx, 2018; Peredo and Pyenson, 2018; de Muizon et al., 2019; Bisconti and Carnevale, 2022; Bisconti et al., 2023).

Moreover, during the Oligocene Epoch, Chaeomysticeti (the toothless mysticetes) emerged, with some of the earliest-diverging species including *Maiabalaena nesbittae* from Oregon in the early Oligocene (Peredo et al., 2018), *Sitsqwayk cornishorum* from Washington in the late Oligocene (Peredo and Uhen, 2016), and *Tlaxcallicetus guaycurae* from Baja California Sur in the late Oligocene (Hernández-Cisneros, 2018). Additionally, other Chaeomysticeti have been described in recent years, including *Horopeta umarere* from New Zealand in the late Oligocene (Tsai and Fordyce, 2015); *Whakakai waipata* from New Zealand in the late Oligocene (Tsai and Fordyce, 2016); and *Toipahautea waitaki* from New Zealand in the early Oligocene (Tsai and Fordyce, 2018).

The most basal family is Eomysticetidae, with records spanning from the early Oligocene to the early Miocene (Sanders and Barnes, 2002a, 2002b; Okazaki, 2012; Boessenecker and Fordyce, 2014, 2015a, 2015b, 2016, 2017). Fossils have been found along the Atlantic coast (Germany and South Carolina) and both Pacific coasts (Mexico, Japan, and New Zealand) (Sanders and Barnes, 2002a; Okazaki, 2012; Boessenecker and Fordyce, 2014, 2016, 2017; Hernández-Cisneros and Nava Sánchez, 2022; Solis-Añorve et al., 2022; Hernández-Cisneros et al., 2024).

Two Oligocene formations have been recorded in Baja California Sur, Mexico: the San Gregorio Formation (Figure 1A-D), located around La Purísima–San Isidro, and the El Cien Formation, west of La Paz (Hausback, 1984; McLean et al., 1987 Schwennicke, 1994; Fischer et al., 1995). The depositional environment for the San Gregorio Formation has been interpreted from planktic foraminifers and trace fossils as being in water depths of approximately 200 meters (Hausback, 1984; McLean et al., 1984, 1987; Grimm and Föllmi, 1994).

In the present work, we describe the first Eomysticetidae from the late Oligocene San Gregorio Formation in the area around La Purísima–San Isidro, Mexico. *Cochimicetus convexus* gen. et sp. nov. has a partially complete skull with a length of 147 cm, along with both mandibles and tympanic bulla. So far, this is the most complete skull from the Oligocene in Baja California Sur.

MATERIAL AND METHODS

The specimen was mechanically prepared with odontological tools and a pneumatic air scribe. Both the skull and mandibles were consolidated with methyl methacrylate (Paraloid-72) diluted with acetone (propanone). Anatomical description follows Okazaki (2012), Boessencker and Fordyce (2016), Mead and Fordyce (2009), and for the hyoid bones Omura (1964). Measurements of the skull, mandibles, and tympanic bullae can be found in Tables 1–2.

Photographic material was obtained using a Nikon D3300 camera. The photographs were taken with the Photostacking technique (Bercovici et al., 2009) to improve the focus coverage. Furthermore, the images were taken based on the anatomical position and were later chosen and edited in Photoshop v.10. Finally, drawings were made by highlighting the diagnostic structures of the material using Inkscape software. For more detailed photographs of the ventral and lateral regions of the jaws, see Figures S1–S3 in the Appendix).

Cochimicetus convexus was coded into the Fordyce and Marx (2018) matrix, consisting of 275 morphological characters coded for 109 terminal taxa. The sample was expanded with the inclusion of *Kaaucetus thesaurus, Borealodon osedax, Nipa-*
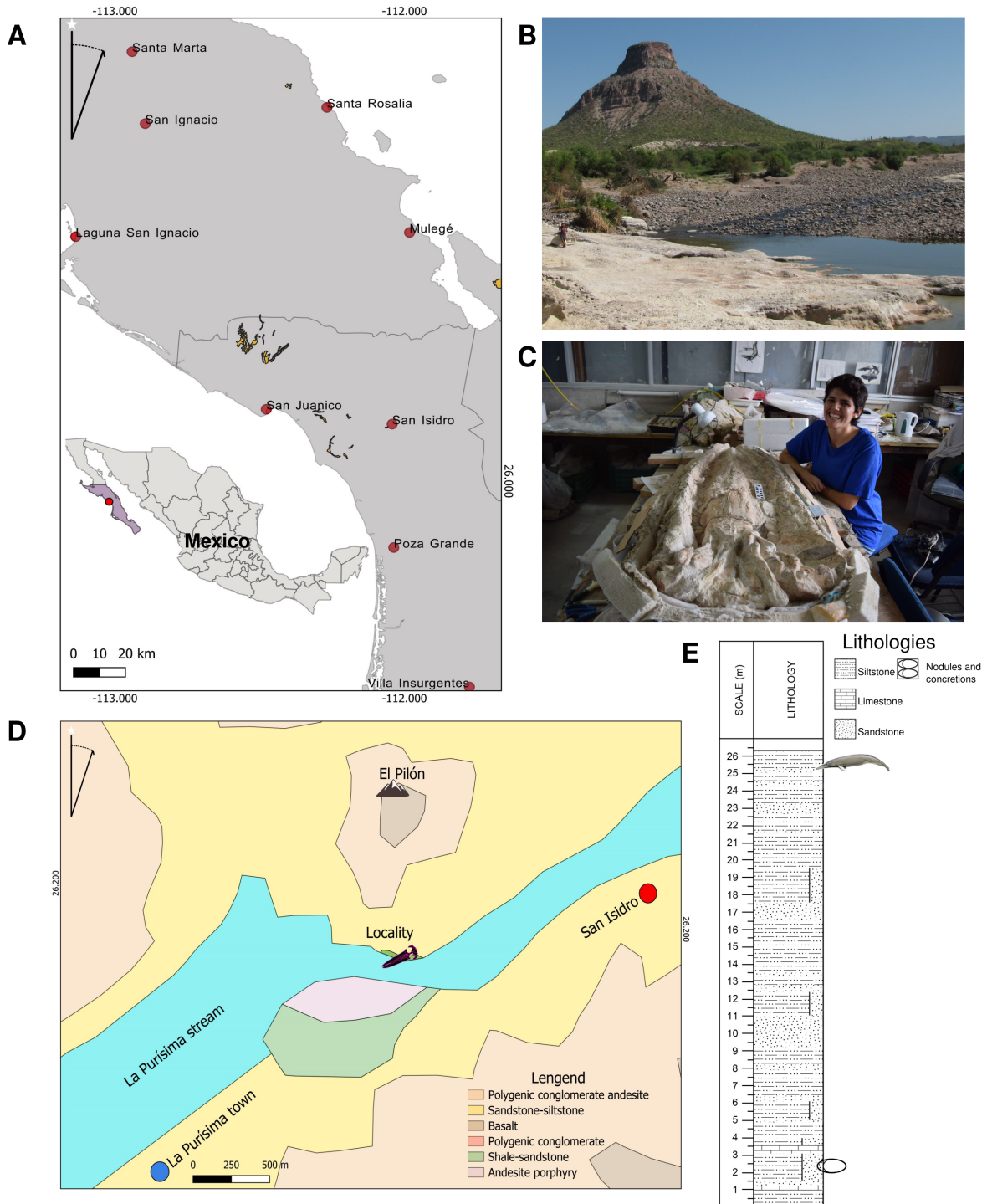
FIGURE 1. Map of the study area. **A,** the studied locality in the state of Baja California Sur in Mexico, zooming in on the area of the municipality of Comondú, where we can find the town of San Isidro. **B,** El Pilón plateau, located in La Purísima–San Isidro, where we can see the La Purísima stream and on the ground the strata where *Cochimicetus convexus* was collected. **C,** the photo shows *C. convexus* in ventral view and Cielo, who prepared the type specimen. **D,** map with close-up of the La Purísima–San Isidro region, the skull represents where *C. convexus* was collected in the fossiliferous sediments near the La Purísima stream. **E,** stratigraphy taken and modified from McLean et al. (1987), is observed on the upper horizon where *C. convexus* was collected. Illustration of Eomysticetidae modified and taken by Carl Buell.

TABLE 1. Measurements of the skull, rostrum, and tympanic bulla of *Cochimicetus convexus*.

Measurement	Value, cm
Condylobasal length	147
Premaxilla length	100.5
Greatest transverse width of premaxilla	18
Transverse width of premaxilla at nasal	13.2
Transverse width of bone nasal	7
Maxilla length	97
Greatest width of maxilla (preserved)	7.5
Anteroposterior length of temporal fossa, frontal to nuchal crest	19*
Length of parietal, occipital apex to frontoparietal suture	25
Bizygomatic width	51
Transverse width of squamosal at level of the glenoid fossa	48*
Exoccipital width	38
Anteroposterior thickness of paroccipital process	4.7
Width of basioccipital crest	19
Nasal length	27*
Transverse width of anteriormost nasal	6
Transverse width of posteriormost nasal	6.3
Preorbital width of frontal	44.3*
Anteroposterior length of supraorbital process as preserved	9.6
Anteroposterior length of temporal fossa, frontal to subtemporal crest	26*
Occipital shield width	11.5
Width across occipital condyles	14.7
Width of foramen magnum	5.8
Anteroposterior length, exoccipital to anterior margin of supraorbital process	43
Anteroposterior length, postglenoid process to anterior margin of supraorbital process	34.2
Anteroposterior length of occipital	23
Length of the tympanic bulla measured at midpoint	6.2
Width of the tympanic bulla measured at the lateral furrow	3.8
Width of the tympanic bulla measured in the anterior region	3.1
Width of the tympanic bulla measured in the posterior region	4.2
Length of the tympanic bulla measured from the most prominent point of the external prominence	6.4

TABLE 2. Measurements of the mandibles of *Cochimicetus convexus*.

Measurement	Value, cm
Total length as preserved	139
Dorsoventral depth at the coronoid process	8
Greatest depth anteriorly	3.5
Length of mandible anterior to coronoid	107
Dorsoventral depth of mandibular foramen	4

rajacetus palmadentis, Salishicetus meadi, Aetiocetus tomitai, Sitsqwayk cornishorum, Maiabalaena nesbittae, Tlaxcallicetus guaycurae, Echericetus novellus, and the taxon described herein (Barnes et al., 1994; Peredo and Uhen, 2016; Hernández-Cisneros, 2018; Peredo and Pyenson, 2018; Peredo et al., 2018; Solis-Añorve et al., 2019; Hernández-Cisneros and Nava Sánchez, 2022; Hernández-Cisneros et al., 2024). Additionally, unpublished data from the tympanic bulla and periotic complex of *Niparajacetus palmadentis* were included in the matrix. Cladistic analysis was performed in TNT 1.1 (Goloboff et al., 2008; Goloboff and Morales, 2023) using the "new technology search", equal weights, and implied weighting with constant $K = 6$ and $K = 12$. Analyses included 10,000 random addition sequences and tree bisection-reconnection branch swamping that saved 10 trees per replicate (view Figure S4). Node support was calculated in TNT by bootstrap (1000 replicates with default parameters). We reported a strict consensus tree with branch support. In addition, a tree was generated with bootstrap support. The tree obtained was visualized in Mesquite 2.75 software (Maddison and Maddison, 2023), where we were able to visualize a map of synapomorphies. Finally, editing of the trees was carried out in Figtree v1 software 4.4 (Kalinowski, 2009).

Institutional abbreviations. MHN-UABCS, Museo de Historia Natural de la Universidad Autónoma de Baja California Sur, La Paz, Baja California Sur, México. **IGM**, Instituto de Geología, Universidad Nacional Autónoma de México, México.

SYSTEMATIC PALEONTOLOGY

Order CETACEA Brisson, 1762
Clade PELAGICETI Uhen, 2008
Clade NEOCETI Fordyce and de Muizon, 2001
Suborder MYSTICETI Flower, 1864
Unranked CHAEOMYSTICETI Mitchell, 1989

Family EOMYSTICETIDAE Sanders and Barnes, 2002
Genus *COCHIMICETUS* gen. nov.

zoobank.org/3744E5DB-17F4-4814-AF4A-9785A0A5C9AD

Cochimicetus convexus gen. et sp. nov.

zoobank.org/1ADB9465-8C21-4637-8198-ACBDC3B98FD7

Etymology. *Cochimi* from the indigenous nomads from north of Baja California Sur, combined with *cetus*, the Latin word for "whale". *Convexus* is a word in Latin that means convex form; it is illustrated in the anterior tip of the tympanic bulla, which differs from the pointed shape of other eomysticetids.

Holotype. MHN-UABCS-Sg6/71/208, with a slightly fragmented cranium and mandibles, was collected by Gerardo González Barba, Alberto Epelboim Jarovinsky, José Alberto David Aguilera, Ali González G., A. Ehecatl H. Cisneros, and F. Garza in 2011. This specimen is stored in the Paleontological Collection of Vertebrates at the Universidad Autónoma de Baja California Sur, Mexico.

Diagnosis. *Cochimicetus convexus* is classified as a Neoceti based on several derived characteristics: a partially open mesorostral groove; an anteroposteriorly elongated rostral portion of the maxilla; the presence of an anteorbital process of the maxilla; an anterodorsally inclined supraoccipital shield; and a narrow intertemporal region. It is further identified as a Mysticeti due to specific features, including the dorsoventrally thin posterolateral region of the maxilla on the rostrum; the apex of the zygomatic process of the squamosal closely opposed to the postorbital process of the frontal; and an external occipital crest restricted to the anterodorsal half of the supraoccipital shield. *Cochimicetus convexus* and eomysticetids differ from toothed mysticetes in their lack of large emergent teeth during adulthood, as well as in having a significantly elongated rostrum and a kinetic maxilla. Additionally, *C. convexus* differs from *Maibalaena nesbittae* in lacking frontal-parietal sutures that converge posteriorly, with the frontals penetrating between the parietals. The posterior border of the nasal is not aligned with the preorbital level. Furthermore, it diverges in the apex of its occipital shield, which represents the highest point of the skull, and in the triangular coronoid process of the mandible, which is anteroposteriorly longer than it is dorsoventrally tall. *Cochimicetus convexus* also differs from *Sitsqwayk cornishorum* in several ways: it does not have a dorsal surface of the nasals that forms a sagittal keel; it lacks an external occipital crest preserved as a blunt ridge that

divides the anterior half of the occipital shield into two dorsolaterally sloping facets; there is no tympanic bulla in the lateral lobe extending posteriorly to the medial lobe, with the two areas separated by a notch; and it possesses a mandibular condyle and neck that are medially curved, giving the mandible a sinusoidal profile in dorsal view. *Cochimicetus convexus* is identified as a basally branching Eomysticetidae based on the following characteristics: the absence of a postorbital ridge; lack of a supramastoid crest along the entire zygomatic process of the squamosal; a zygomatic process of the squamosal with parallel medial and lateral margins; the development of secondary squamosal fossa; elongated nasals; the inclusion of a frontal with anteromedial projection; and an anteroposteriorly long and transversely narrow intertemporal region with an oval temporal fossa (longer anteroposteriorly than transversely wide). *Cochimicetus convexus* differs from all Eomysticetidae in the following combination of attributes: the tympanic bulla anterior tip is round in the dorsal or medial view and diverges from the pointed shape in other eomysticetids; it has a pronounced parietal squamosal suture; in the tympanic bulla, the orientation of the lateral furrow is anteroventrally orientated; the tympanic bulla position of the main ridge in the ventral view is the medial and lateral sides of the bulla; in the maxilla, nutrient foramina, and sulci are absent; the medial contact of the premaxilla along 2/3 of the rostrum is mostly separated from the rostrum and is medially fused from the anterior tip; the anteorbital notch is absent; and the external occipital ridge is absent.

Locality. The skull of *Cochimicetus convexus* was collected near Mount "Pilón", situated between the towns of San Isidro and La Purísima (26°11'51.036"N, 112°3'28.800"W) in Baja California Sur, Mexico. This area is part of the San Gregorio Formation (late Oligocene, Chattian, 27.2–23.4 Ma), which consists of a sequence of interbedded phosphatic siliceous shale, diatomite, pelletoidal phosphatic sandstone, and rhyolite tuff. An age of 25 Ma was determined by Hausback (1984) using K–Ar radiometric methods on biotite from a tuff bed at Arroyo San Hilario. Additionally, four other tuffs in the San Gregorio Formation in the La Purísima area yielded K–Ar dates ranging from 27.2 to 22 Ma. On the other hand, evidence of diatomite indicates a late Oligocene–early Miocene age in the La Purísima area (McLean et al., 1987). The specimen was found exposed at a depth of 25 m within a sequence interbedded with pelletoidal sandstone, siliceous shale, and phosphatic conglomer-
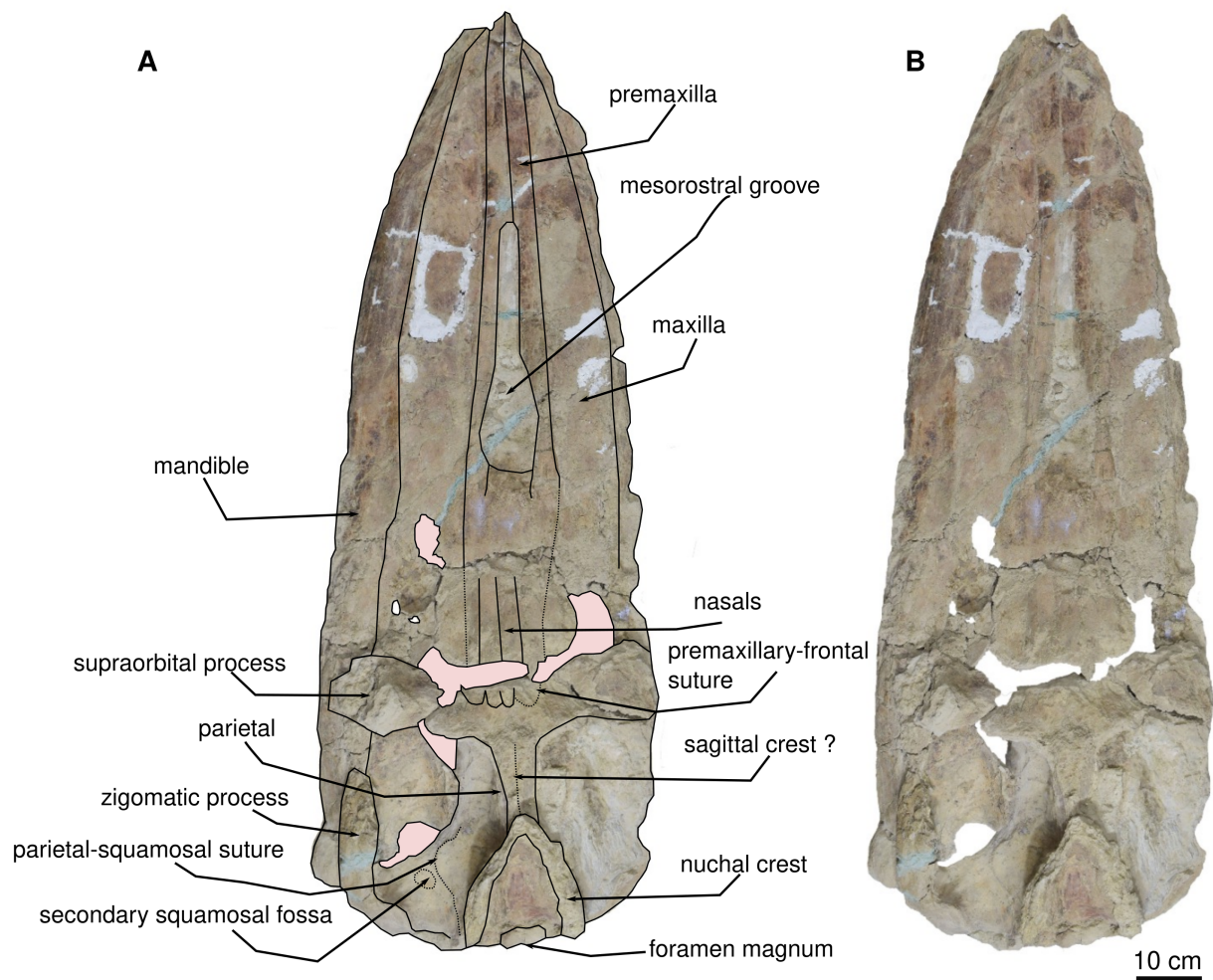
FIGURE 2. Dorsal view of the holotype of *Cochimicetus convexus*. **A,** image showing the identified structures. **B,** photography with scale 10 cm.

ate (Figure 1E). Finally, Föllmi et al. (2019) obtained LA-ICP-MS zircon ages from the volcanic ash layers, which range between 27.84 and 21.21 Ma.

Description

Cochimicetus convexus is a relatively well-preserved skull with two fragmented mandibles fused to the cranium (Figure 2). Nevertheless, it has diagnostic elements. The total condylobasal length is 147 cm, and the bizygomatic width is 51 cm. The occipital shield is trefoil-shaped, without a crest, and has two tympanic bullae *in situ*; the left bulla was not included in the description.

Rostrum. In both dorsal and ventral views, the skull is fragmented in the rostral region, which complicates the visibility of the sutures, while the posterior region is well preserved (Figures 3–4). In the ventral view, a palatal keel is formed by the

vomer, and the medial margins of the maxilla are well developed in the rostral area. The maxilla is clearly visible from the ventral view, although the contact with the palatine is not very discernible due to the presence of fractures. Nevertheless, it can be inferred that the parietal suture exhibits an irregular shape in the anterior region of the basicranium.

In the anterior portion of the rostrum, it is difficult to identify the protrusion of the premaxilla, as this area is eroded in the ventral view. The vomer is exposed along the length of the rostrum, becoming more prominent in the anterior region. Posteriorly, the crest of the vomer is well defined, high (Figure 3), and narrow at the edges, with its most posterior point located anterior to the edge of the pterygoid of the hamulus.

Maxilla. In the dorsal view, the premaxilla extends beyond the maxilla. From the most anterior edge,
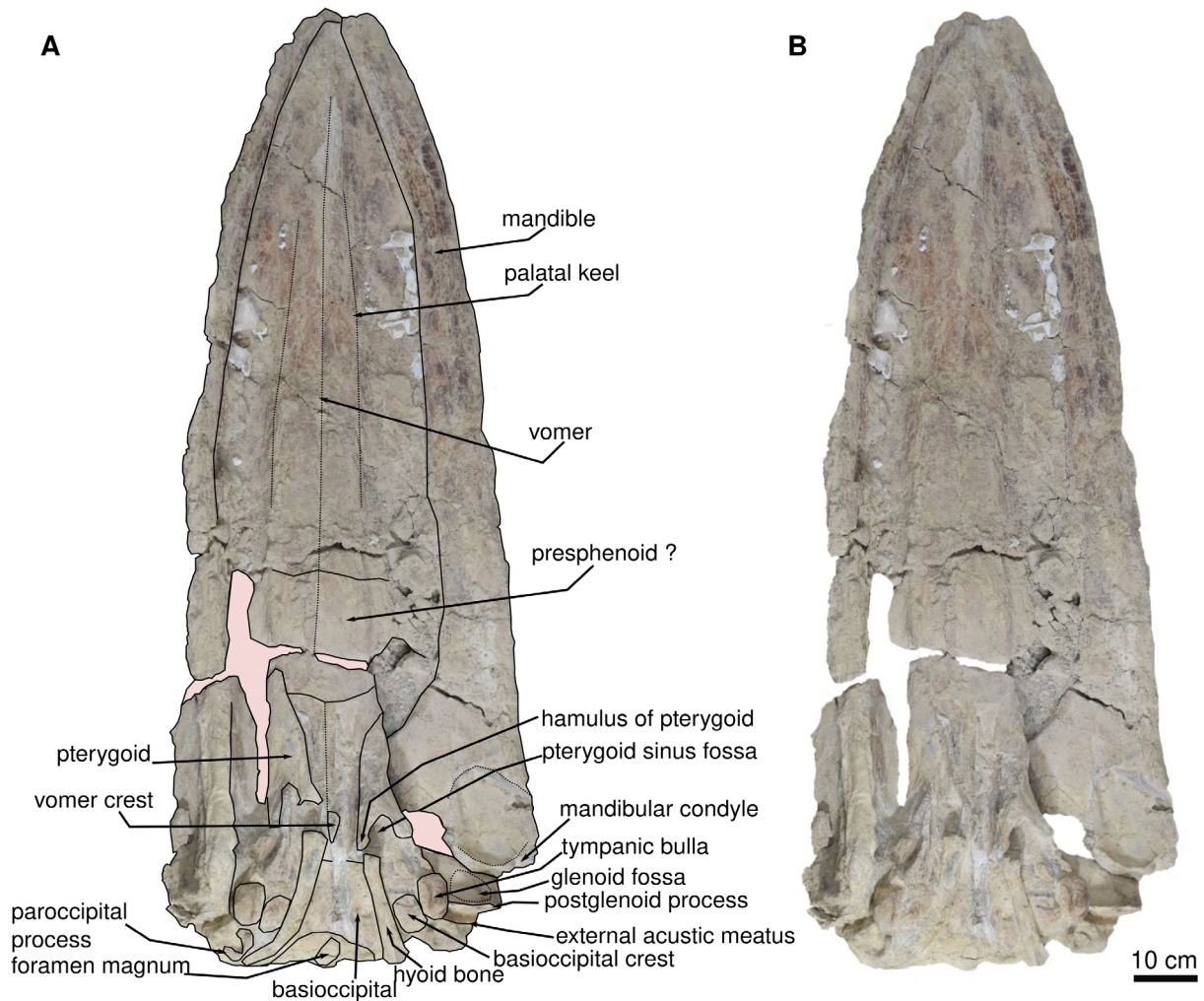
A

B

FIGURE 3. Ventral view of the holotype of *Cochimicetus convexus*. **A,** image showing the identified structures. **B,** photography with scale 10 cm.

the maxilla is flat (Figure 2), narrow, and widens anterolaterally with a concave margin lateral. The contact between the frontals and the maxilla is unknown, but the left maxilla presents an exposure with the frontal supraorbital process; the ascending process of the maxilla is moderately long. In the ventral view, the maxilla's both sides are very fragile and heavily eroded. The maxilla is narrow at its anterior edge and widens anterolaterally. Additionally, there is no visible foramina or sulci on its surface.

Premaxilla. In the dorsal view, the premaxilla is the anterior-most tip of the rostrum (Figure 2), with a length of 100.5 cm. The premaxilla has a sinuous form, is wide at the anterior and posterior tip, and is mediolaterally narrow around the nasal fossa. The premaxilla is very eroded ventrally.

Nasals. In the dorsal view, the nasals are flat and long (Figure 3), with parallel margins to the naso-frontal suture. In lateral and dorsal views, the nasal suture is visible and "m" shaped. The posterior border of the nasals is at the same level as the pre-maxilla. It is unclear if a fusion with the maxilla exists and is narrower.

Sphenoids and pterygoid. In the ventral view (Figures 4–5), the basisphenoid is damaged, and the alisphenoid is not exposed. However, the pterygoid has a semi triangular form and a deep sinus foramen. The best-preserved pterygoid is the left one, while the right pterygoid shows only fragments of the pterygoid hamulus. In general, the pterygoid is broad and long. It has a wide sinus fossa. The pterygoid hamulus is posteriorly directed and well developed in a finger shape.
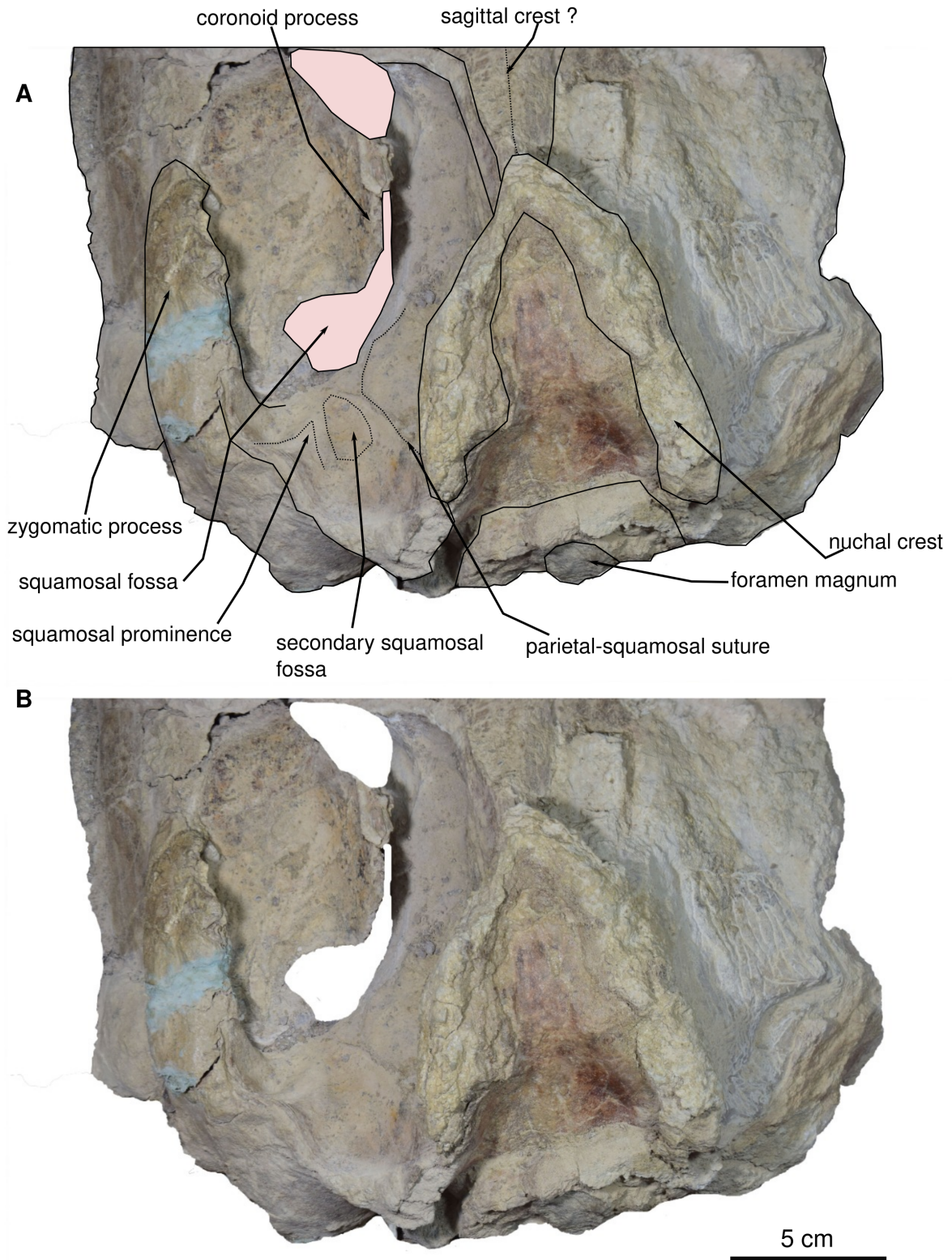
FIGURE 4. The cranial region and its structures in detail in dorsal view. **A,** each structure identified in this region is indicated. **B,** photography of *Cochimicetus convexus,* scale 5 cm.

Frontals. In the dorsal view, the premaxilla-nasofrontal and nasofrontal suture are corrugated. Only the left part is preserved (Figures 3, 5). The lateral view, it has a triangular shape, but the preorbital and postorbital processes are lost, and probably has no alveoli or foramina either. A slight remnant of a broken orbitotemporal crest, on the left edge of the anterior margin of the supraorbital process for the frontal, continues until the middle of the supraorbital process of the frontal.

Parietals. In the dorsal view, the parietals are long from the anterior margin of the occipital to the fronto-parietal suture (Figures 3, 5). The intertemporal region is constricted, and presumably, there is a thin, short sagittal crest, but poor preservation does not allow for certainty. The temporals are thick and concave, which is why they are oversized in the intertemporal region. The nuchal crest extends over the parietals but does not layer over the temporal fossa and is the most elevated point. The temporal fossa are larger than they are wider and have a notable subtemporal crest.

Squamosal. In the dorsal view, the posterior margin of the squamosal fossa extends laterally to the supramastoid crest; it does not extend to the tip of the zygomatic process due to the presence of the squamosal prominence (Figures 3–4). The parietal-squamosal suture is prominent and elongated and ends in the subtemporal crest. In the lateral view, the suture of the squamosal and parietal descend to approximately the level of the posteriormost region of the pterygoid at its lateral border. The zygomatic process is well preserved (left side) and elongated, with a cylindrical shape (anteroposteriorly) slightly bent anterolaterally. The secondary fossa of the squamosal is at the end of the ridge formed by the squamosal prominence; it is circular and shallow (Figure 4).

In the ventral view (Figures 5–6), the disruption of the mandible does not allow us to observe the total length of the glenoid fossa; thus, it cannot be measured. The glenoid fossa is subtly concave, and the postglenoid process is vertical with a superior semicircular margin. It is concave in the lateral view, and from the superior tip, it becomes thick towards the bottom.

Basioccipital and stylohyoid. In the ventral view, the basioccipital is broad, compared to the basisphenoid, and the basioccipital has a fracture in the middle, while the suture of the basioccipital can be seen laterally with a straight shape (Figures 4, 7). The left basioccipital crest is exposed with a slightly oval and robust shape, with a straight lateral border and a convex medial border. The right basioccipital crest is inconspicuous because the stylohyoid, together with the tympanic bulla, has pushed it to the lateral border. Above these are the stylohyoid bones. No other bones of the hyoid apparatus were found, but the position of the stylohyoid is considered natural. Stylohyoids are long and robust with a length of about 20 cm and a width of 3.5 cm measured medially. The stylohyoids are located on the basioccipital.

Supraoccipital and exoccipital. In the dorsal view, the supraoccipital is triangular and lower than the nuchal crests; it has no external ridge. The occipital shield is trefoil-shaped due to concave tubercles (in the posterior view), and it has no ridge dividing it into two halves; it is about 11.5 cm wide (Figures 4, 7). The occipital condyles are rounded but eroded, but in the dorsal view, they protrude from the skull, although not very far (14.7 cm). The foramen magnum is rounded 5.8 cm. In the posterior view, the exoccipital is small compared to the squamosal (in the posterior view), with a width of 38 cm. In the ventral view, the paroccipital is well exposed on the right side, and it lies well anterior to the occipital condyles and has a ventral direction. It is thin at its margin.

Tympanic bulla. The tympanic bulla was found in situ (Figures 5–6) and was subsequently removed with great care for a more thorough analysis. In the dorsal view, the tympanic bulla has is pear-shaped, with a rounded anterior tip that widens posteriorly. In the posterior view, the elliptical foramen is not visible due to erosion in that region (Figure 7). The lateral lobe extends further posteriorly than the medial lobe, with both lobes separated by a notch. Along the outer margin of the medial lobe, the ventromedial ridge is prominent, extending almost 75% of the total length. A median furrow is incised in the posterior part of the lateral lobe and continues straight to the middle section of the tympanic bulla.

In the ventral view, the anterior and posterior pedicles are indicated by small fragments. The tympanic bulla appears elongated in the lateral view, with a rounded anterior tip. The anterior and posterior parts are somewhat proportional, but the posterior part is more pronounced, featuring a well-defined lateral furrow. The sigmoid process is located further posteriorly, curving slightly within the lateral furrow and extending much further back within the bulla. The overlaps in the posterior portion of the lateral lobe are also rounded.

In the medial view, the involucrum is narrow at the anterior end, and the dorsal margin is mostly smooth, with creases along its edge. At the most
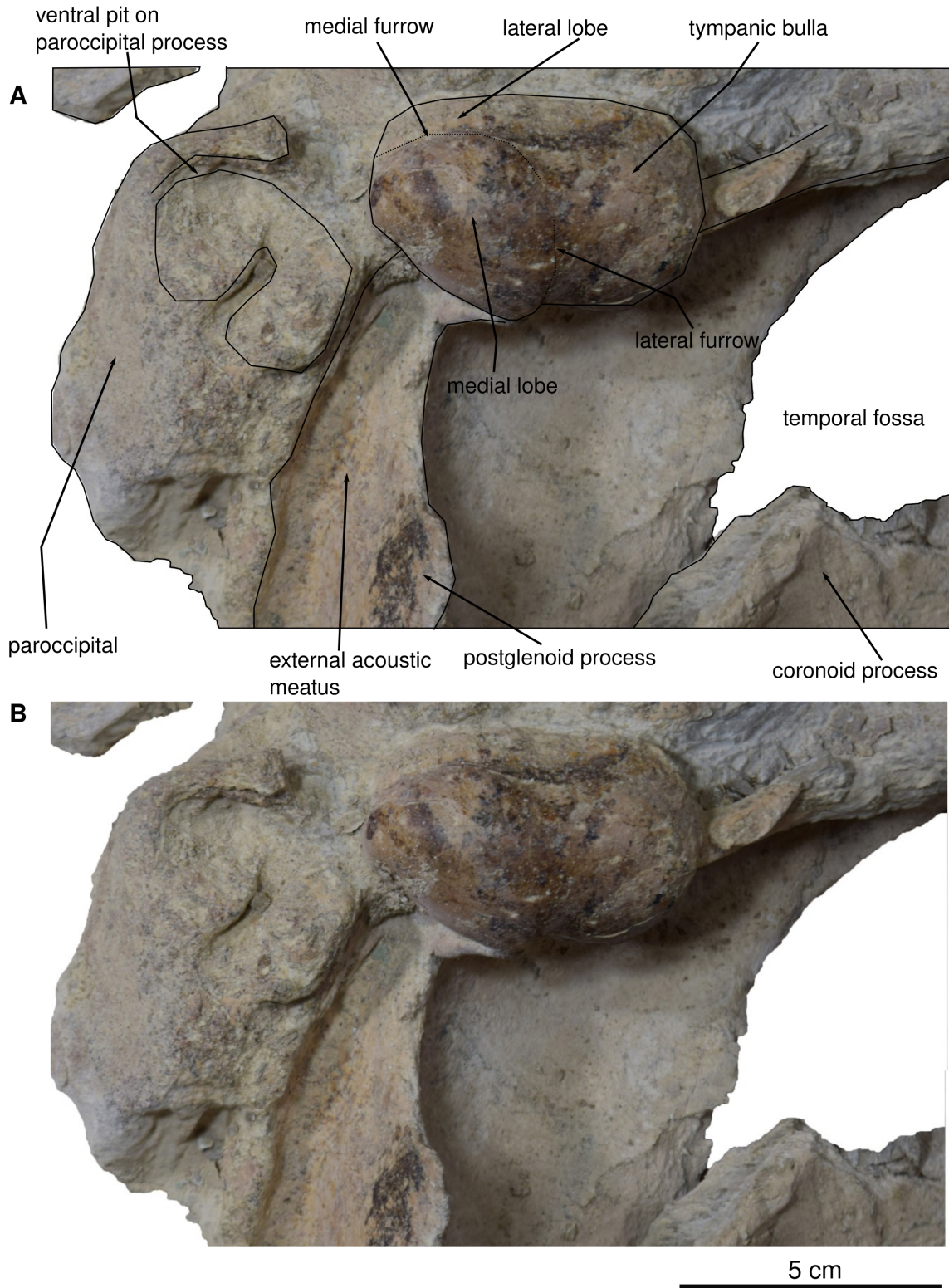
FIGURE 5. Close-up of the ear area in ventral view. **A,** photography of *Cochimicetus convexus*. **B,** image showing the undefined structures with a scale 5 cm.
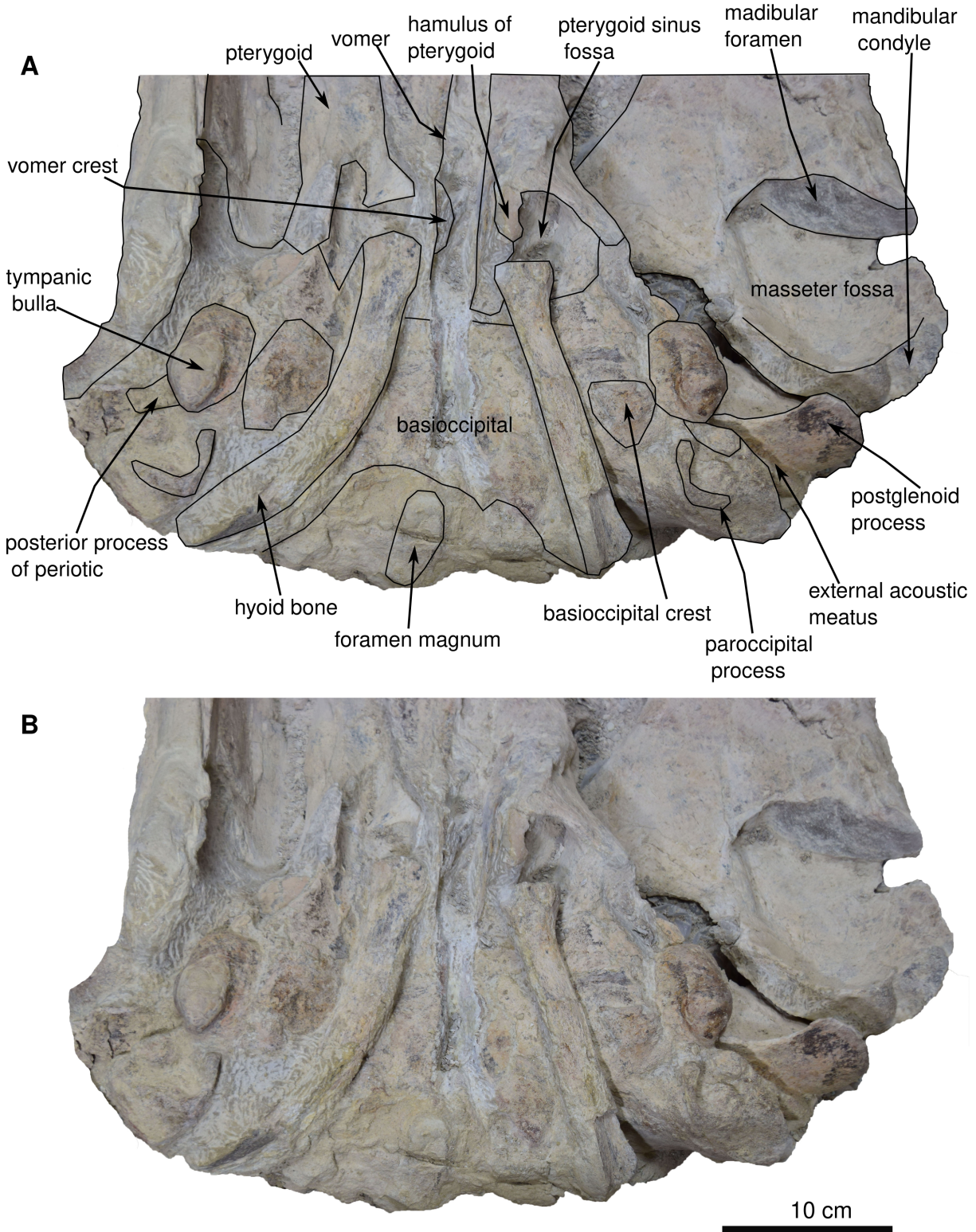
FIGURE 6. Close-up of the cranial case in ventral view. **A,** photography of *Cochimicetus convexus*. **B,** image showing the undefined structures with a 10 cm scale.
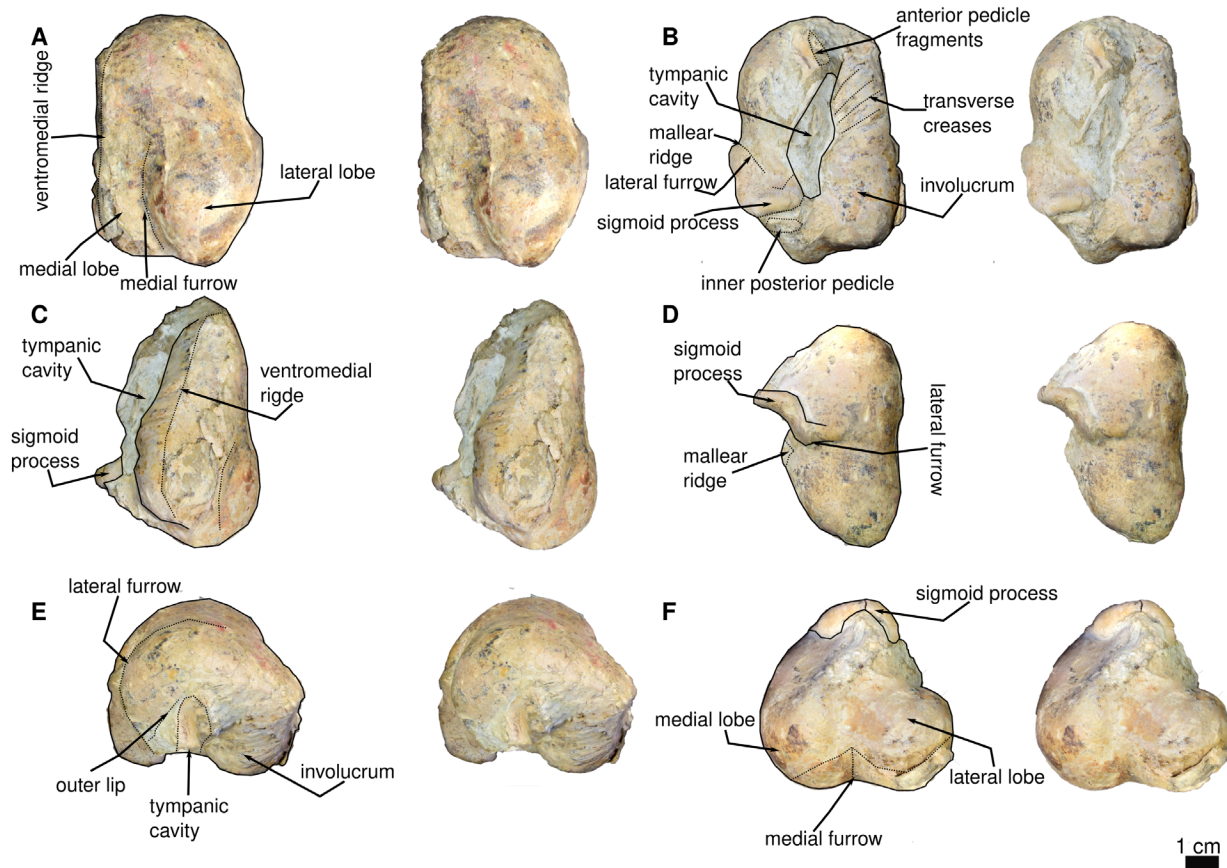
FIGURE 7. Left tympanic bulla in dorsal (A), ventral (B), medial (C), lateral (D), anterior (E), and posterior (F) view, with a scale of 1 cm.

posterior part, the dorsal margin exhibits a "step" that transitions into a bulbous section. The sigmoid process is positioned immediately posterior to the outer posterior pedicle, while the inner posterior pedicle is closely compacted with the median furrow. Importantly, the tympanic bulla was carefully extracted using an air script, leaving remnants still visible in the skull. As observed in the lateral view and the medial furrow in the posterior view, both lobes share similar widths, as well as the shapes of the inner lip/tip and posterior pedicle.

Mandibles. Both mandibles are preserved *in situ*, although the left mandible, which is approximately 139 cm long, is better preserved. It has several fractures along its body (Figure 3).

In general, the mandible in the dorsal view has a slight medially directed curvature, and the curvature is mainly observed in the middle and distal regions of the mandible. The mandible in the medial or lateral view narrows at the anterior region and widens in the posterior region. In the ventral view, the mandibular foramen is observed to be wide; it is wider anteroposteriorly than it is high. The mandibular condyle is visible in the posterior or medial view, and its posterior edge is rounded and broad. The neck of the mandible is concave, forming the coronoid process at the top. The coronoid process is eroded in the upper region, but it is possible to trace the convex and rounded shape of the edge of the coronoid process, which shows no posterior deviation. In the dorsal view, the coronoid process has a medial displacement. In the lateral view, a mental foramen is visible in the anterior part of the mandible (see Figures S1–S2).

PHYLOGENETIC ANALYSIS

We show our interpretations found with "new technology search" with 10,000 random addition sequences with equal weights (Figure 8). Furthermore, we obtained 77 trees with a length of 1,410, CI 0.262, and RI 0.748. Meanwhile, we used implied weightings with constant K= 6 and K = 12
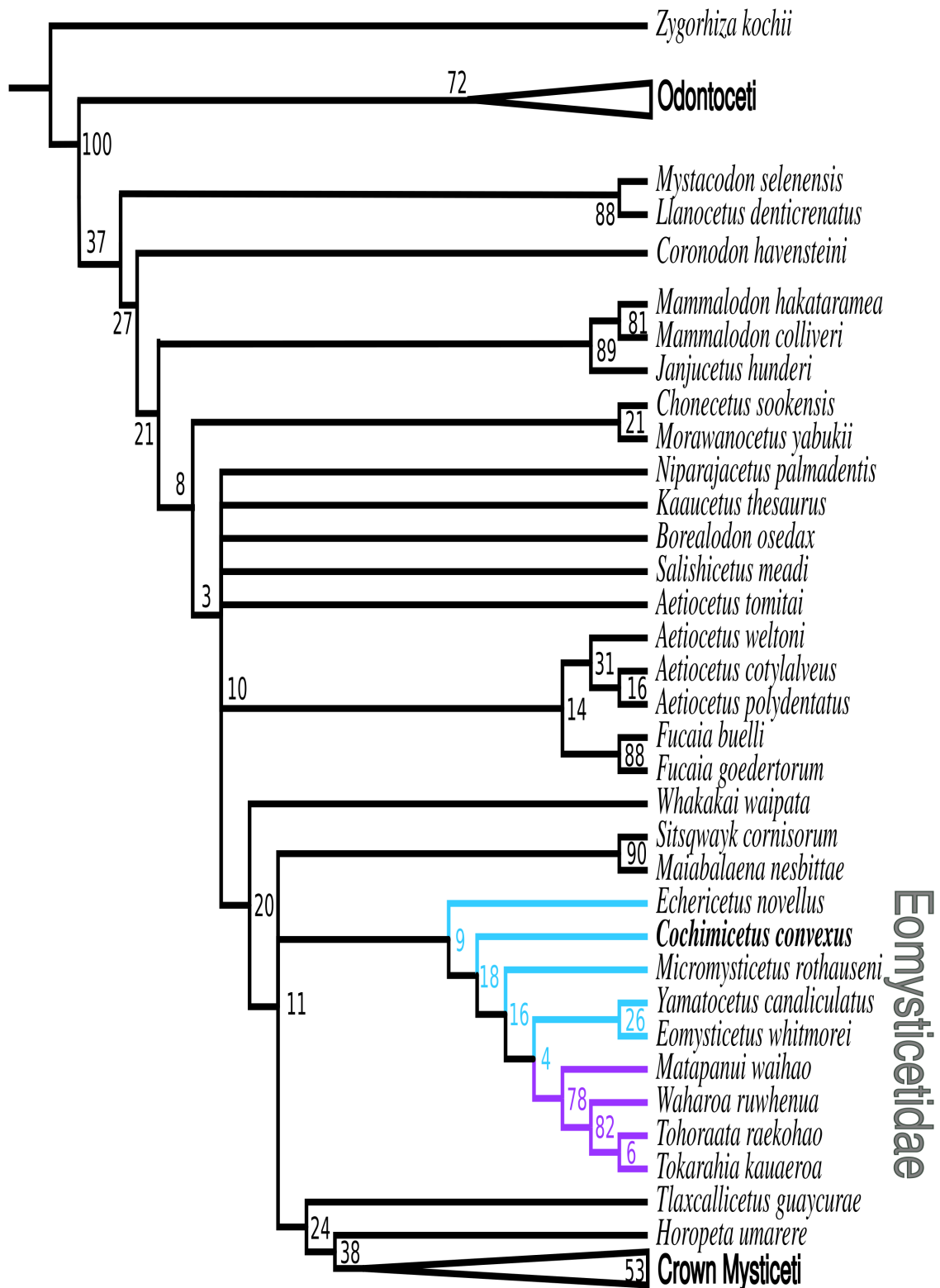
FIGURE 8. Phylogenetic analysis showing the recovery of *Cochimicetus convexus* to Eomysticetidae. Blue shows the northern hemisphere Eomysticetids assemblage and purple shows the southern hemisphere assemblage. Show the equal weights, show the consensus tree with CI: 0.262; RI: 0.0.748; 1,410 total lengths.

(Figure S4). About K = 6, we obtained one tree with a length of 89.35148, CI 0.259, and RI 0.745. Finally, with K= 12, one tree had a length of 57.74474, CI 0. 261, and RI 0.747 (Figure S4). Bootstrap support differed in each hypothesis but low, with implied weights *Cochimicetus convexus* has a support of 18, implied weights K = 6 with 23, and K =12 with 14 support. It is important to mention that the different hypotheses shown in this work present a low bootstrap support as many taxa present a high homoplasy gradient, mainly due to lack of data or incomplete materials.

The monophyletic clade of Eomysticetidae is conserved in the different hypotheses of equal weights (Figure 8) and implied weights of K= 6 and K=12 (Figure S4), as proposed by different authors such as Boessenecker and Fordyce (2015a, 2015b), Marx et al. (2019), and Boessenecker et al. (2023). However, this differs from the alternative hypothesis of Bisconti et al. (2023) where *Maiabalaena nesbittae* and *Sitsqwayk cornishorum* are considered as belonging to two different clades with *M. nesbittae* being part of a primitive clade and *S. cornishorum* as a sister group of Balaenomorpha together with *Horopeta umarere*. In our analysis, equal weights and implied weights support the monophyletic group of Eomysticetidae with the following combination of characteristics: outline of frontoparietal suture is lobate (83: state 0); the supramastoid crest of zygomatic process of squamosal is absent (100: state 2); transverse width of squamosal lateral to exoccipital is a width equal to or greater than 15% of the distance between the sagittal plane and the lateral edge of the exoccipital (104: state 0); coronoid process in lateral view has formed a broad plate (229: 0); anterior outline of coronoid process is bent laterally (231: state 1); and shape of the coronoid process in the medial view is bluntly triangular and considerably longer than high (234: state 1).

All three hypotheses of our results show *Cochimicetus convexus* at the basally branching of the *Yamatocetus canaliculatus, Eomysticetus whitmorei, Micromysticetus rothauseni, Matapanui waihao, Waharoa ruwhenua, Tokarahia kauaeroa,* and *Tohoraata raekohao*. According to the analysis, *C. convexus* differs from these taxa mentioned by the following combination of characteristics: length of the rostral portion of maxilla anterior to antorbital notch is more than one and a half times the bizygomatic width (1: state 2); outline of frontoparietal suture is highly irregular (83: state 2); ventromedial corner of paroccipital process in posterior view (134: state 0); posteriormost point of the paro-

ccipital process is located more anteriorly than the posterior edge of the occipital condyle (135: state 0).

However, *Cochimicetus convexus* is not the most basally branching denoting taxon in the family Eomysticetidae. In our analysis of equal weights and implied weights, *Echericetus novellus* is observed to be the most early-diverging taxon in the family.

It is important to note that *Sitsqwayk cornisorum* and *Maiabalaena nesbittae* do not belong to the family Eomysticetidae due to the following combination of characters: the shape of pterygoid hamulus is expanded into a dorsoventrally flattened plate flooring the pterygoid sinus fossa (125: state 1); in the ventral view, the ventral border of sagittal part of vomer (nasal septum) in traverse line with or anterior to the anterior half of the tympanic bulla (127: state 2), and a mandibular body in medial view increasing in height anteriorly (221: state 4).

DISCUSSION

Eomysticetids from Baja California Sur, Mexico

Chaeomysticeti is an infraorder of baleen whales characterized by the absence of functional teeth in adults (Boessenecker and Fordyce, 2015a; Peredo and Uhen, 2016). The most basal members of Chaeomysticeti include the late Oligocene (28–26 Ma) *Sitsqwayk cornishorum* from the Pysht Formation in Washington (Peredo and Uhen, 2016) and the Early Oligocene (33 Ma) *Maiabalaena nesbittae* from the Alsea Formation in Oregon. A notable record for the family Eomysticetidae from the early–late Oligocene (29–27 Ma) in the Jinnobaru Formation, Japan, is *Yamatocetus canaliculatus* (Okazaki, 2012; Boessenecker and Fordyce, 2016).

Informally, basal mysticetes have been reported from Baja California Sur, but no detailed descriptions exist, with only inventory or taxonomic lists available (Applegate, 1986; Barnes, 1998, 2002). In recent years, research on cetaceans in Baja California Sur has intensified, resulting in the description of three eomysticetids from the late Oligocene. These taxa originate from different localities. The first is from Mesa del Tesoro, a site in San Juan de la Costa within the El Cien Formation (Hernández-Cisneros and Nava-Sánchez, 2022), which shows an affinity with the genus *Eomysticetus* sp. The second specimen comes from the same formation at the Ten Minute locality in San

Hilario, identified within the family Eomysticetidae (Solis-Añorve et al., 2022, 2024).

The third specimen, *Echericetus novellus*, is represented by fragments of a skull, facial bones, periotic elements within the matrix, 31 postcranial elements, and a forelimb fragment. This specimen was collected northwest of Rancho La Palma and northeast of Cerro El Divisadero in La Paz, with an estimated age slightly older than 27.95 Ma, from the latest Rupelian (Hernández-Cisneros et al., 2024). However, due to the poor preservation of these materials, precise classification at the species level remains challenging.

The description of *Cochimicetus convexus* is particularly significant due to its well-preserved diagnostic elements. Additionally, it is the first taxon described from the late Oligocene San Gregorio Formation in the La Purísima–San Isidro area.

Phylogenetic Position and Morphological Comparisons

Cochimicetus convexus differs from *Eomysticetus whitmorei* in that the latter lacks a thin interparietal, which is wider in *C. convexus.* The anterior region of the tympanic bulla is dotted, it does not have thick transverse basioccipital ridges, there is an absent facet on the ventral surface of the dorsolateral external of the zygomatic process, and the exoccipital is located posterior to the occipital condyle.

According to the diagnosis of Sanders and Barnes (2002a), *Cochimicetus convexus* differs from *Eomysticetus carolinensis* in lacking the shorter intertemporal region and in having parietals one-third shorter in length along the midline; *C. convexus* also has an anterior portion of heavily corrugated supraoccipital, narrower squamosal fossa and a zygomatic process of squamosal that is thinner and more divergent from the sagittal plane. *C. convexus* contrasts with *Micromysticetus tobieni* in the following attributes: it is a small specimen; the lateral margins of the supraoccipital are almost straight in the anterior two-thirds; and the inner margins of the basioccipital crests are rounded and curve away from each other posteriorly, and the space between them is slightly convex (Sanders and Barnes, 2002a).

Cochimicetus convexus differs from *Micromysticetus rothauseni* based on the following: it lacks a cranium with a more rounded posterior margin of the squamosal fossa; the crest on the supraoccipital does not extend close to the dorsal margin of the foramen magnum; the lateral margin

of the occipital shield is more convex; and the basioccipital crests are angular (Sanders and Barnes, 2002a).

Regarding the Eomysticetidae described for Baja California Sur from the late Oligocene El Cien Formation, these are poorly preserved materials, and many of the diagnostic characters are missing. However, *Eomysticetus* sp. (MHN-UABCS-EcSj1/29/142) differs from *Cochimicetus convexus* by the lack of a thickening of the nasal ridges, and they have a broad premaxilla with an ascending process extended farther than the posterior ending of the nasals (Hernadez-Cisneros and Nava-Sánchez, 2022). Moreover, *Eomysticetus* sp. (IGM 7756) differs from *C. convexus* in that the posterior limit of the nasals is anterior to the posterior limit of the maxilla, and the basioccipital ridges are rounded at both ends (Solis-Añorve et al., 2022, 2024). *Cochimicetus convexus* diverges from *Echericetus novellus* in the following characteristics: its mandible is S-shaped in the lateral view; the basioccipital region is wider transversely and anterolaterally; and the ventral region of the mandible is straight, not curved (Hernández-Cisneros et al., 2024).

Meanwhile, the example from the southern hemisphere has the largest fossil record so far. According to the phylogenetic analysis presented in this paper (Figure 8), the southern hemisphere assembly differs from the northern hemisphere's in the following combination of features: the occipital posterior margin of the exoccipital is posteriorly convex and bulbous; the mandibular terminus is spear-shaped in the lateral view; and the anterior region of the tympanic bulla in the dorsal or ventral view is pointed.

Tohoraata raekohao differs from *Cochimicetus convexus* in that it has the following combination of characteristics: a tympanic cavity divided by a transverse ridge; a thickened paroccipital process; a prominently well-developed horizontal cleft; an external prominence of the tympanic bulla that is more protuberant and defined than the internal prominence (Boessenecker and Fordyce, 2014).

Cochimicetus convexus contrasts with the genus *Tokarahia* because it exhibits numerous foramina in the supraorbital process of the frontal; and lateral and medial lobes of the tympanic bulla of equivalent width. Moreover, *Tokarahia lophocephalus* diverges from *C. convexus* in the following attributes: a zygomatic process that does not extend anterior to the occipital shield; more extremely telescoped nasal and premaxilla that penetrate the posterior half of the frontal; and a

tympanic bulla without a median furrow incised as a notch in the posterior margin of the tympanic bulla in the dorsal view (Boessenecker and Fordyce, 2015b). Furthermore, *Tokarahia kauaeroa* differs from *C. convexus* in possessing a deeply incised median furrow of the tympanic bulla in the dorsal view.

Cochimicetus convexus diverges from *Matapa waihao* in that its basioccipital ridges are antero-posteriorly more elongated. The external prominence of the tympanic bulla in the ventral view ends in a pointed shape, the glenoid fossa is deep, and the premaxilla extends posterior to the nasal (Boessenecker and Fordyce, 2016). *Waharoa ruwhenua* is different from *C. convexus* as follows: the anterior region of the zygomatic process is thinner; the nuchal ridges are not thickened; the squamosal fossa is widened posteriorly; the orbitotemporal ridge is curved; and the posterior bulla prominences are indistinct in the ventral view (Boessenecker and Fordyce, 2015a).

According to phylogenetic and comparative anatomical analysis, *Echericetus novellus* and *Cochimicetus convexus* represent the most primitive taxa in the Northern Hemisphere assemblage within the family Eomysticetidae. In our analysis (Figure 8), we observed the persistence of its position. However, anatomically, we found similarities with *Yamatocetus canaliculatus* from Japan, but this is not reflected in our systematic analysis, probably due to homoplasy in other individuals with few preserved diagnostic elements. The following is a list of the synapomorphies that it shares with *Y. canaliculatus*: 1) in the premaxilla, the posterior part in the lateral aspect is dorsoventrally shallower or the same depth as anteriorly; 2) in the maxilla and mandible, the dentition and alveolar groove are absent; 3) the nasal length is long, > 40% BZW; 4) the intertemporal constriction with a sagittal crest is a low ridge; 5) the zygomatic shape of the dorsal aspect tapers anteriorly, and mandible and the orientation of the coronoid process are laterally hooked; and 6) broad pterygoid development.

On the contrary, *Cochimicetus convexus* can be distinguished from *Y. canaliculatus* according to the following differences: 1) its tympanic bulla with the anterior region in the dorsal view is oblique; 2) its nuchal ridges are more developed; and 3) it lacks premaxilla that are widened in the anterior region of the rostrum (Okazaki, 2012).

Comments on the Feeding and Diversification of Eomysticetids

In the mandibles, there were no alveoli visible from the dorsal view, indicating a lack of dentition. Eomysticetids are defined within Chaeomysticeti as baleen whales that do not possess functional teeth as adults (Boessenecker and Fordyce, 2016; Peredo and Uhen, 2016). Skull mobility in filter-feeding whales is crucial for their feeding strategies. Generally, there are three types of feeding: skimming, gulping, and benthic suction (Berta et al., 2016; Peredo et al., 2017). However, alternative hypotheses have been proposed regarding the feeding mechanisms of stem mysticetes.

The feeding habits of eomysticetids and Chaeomysticeti remain a complex topic. Here, we can only speculate about the similarities between *Cochimicetus convexus* and the stylohyoid elements of the hyoid apparatus in *Maiabalaena nesbittae* and *Yamatocetus canaliculatus*, both of which are well preserved and complete. These bones are associated with the shape, size, and species distinction of the tongue (Omura, 1964).

Werth (2007) described the stylohyoid elements of *Balaenoptera* as flat and narrow, somewhat thicker in *Megaptera*, and large and cylindrical in balaenids and *Eschrichtius*. Kienle et al. (2015), studying a newborn of the same species, emphasized the importance of tongue size and suction feeding. Peredo et al. (2018) characterized the stylohyoid of *M. nesbittae* as narrow and elongated, lacking an apparent bony connection to the basihyoid. The proximal end is robust and circular in cross-section, gradually tapering and flattening distally, resulting in a more ovoid cross-section at the distal end. These bones were not found in situ. Similarly, Okazaki (2012) noted a stylohyoid or possibly epihyoid with a rod-like form and a flat internal surface; one end is flattened and curved, while the other is triangular in section, measuring 139.8 mm in length. This bone was also not found in situ. In contrast, the stylohyoid bones of *Cochimicetus convexus* were located in their natural anatomical position. These stylohyoids are approximately 20 cm long and cylindrical, featuring a curved and robust anterior end and a flattened posterior end, resembling *M. nesbittae* more closely than *Y. canaliculatus*. Peredo et al. (2018) proposed that suction feeding was likely effective due to a combination of robust hyoid and orofacial morphology, which occluded lateral gape, similar to extant balaenids and beaked whales. Tanaka (2024) suggested hypothetical filter-feeding strategies based on the relationships between the basi-

hyal-thyrohyal form and feeding strategies among both extant and extinct baleen whales. Consequently, *Y. canaliculatus* is closely related to clusters of other potential small prey feeders, such as balaenids, *Caperea marginata*, and *Eschrichtius robustus.* There is insufficient evidence to establish a direct link between the size and form of these bones and the feeding behavior in *C. convexus*. However, the anatomical similarities with *M. nesbittae* and *Y. canaliculatus*, along with their potential relationships in feeding strategies with balaenids (*C. marginata* and *E. robustus*), which likely engaged in suction feeding and presumably targeted small prey, make the possible feeding mechanisms of this whale intriguing.

Finally, the morphological affinities between *Cochimicetus convexus* and the Pacific species *Yamatocetus canaliculatus* and *Matapanui waharao*, as well as the Atlantic species *Micromysticetus rothauseni*, may have been influenced by the climatic and geographic events of the Oligocene, which were quite specific. The Oi-1 glaciation event (Zachos et al., 2001; Westerhold et al., 2020; Tsai, 2023) marked a climatic shift characterized by icehouse, coolhouse, warmhouse, and hothouse effects (Westerhold et al., 2020), leading to a sea-level fall associated with Antarctic glaciation. Regarding the geography of the Eocene–Oligocene (E–O) transition, the Gaarlandia intercontinental bridge between North and South America formed between 35 and 33 Ma. This bridge connected the Greater Antilles and the Aves Ridge, which is geographically positioned parallel to the west of the Lesser Antilles, which had yet to emerge (Iturralde-Vinent and MacPhee, 1999).

The transition between the Rupelian and Chattian stages coincided with an even greater sea-level fall than the E–O event, resulting in the erosion of global stratigraphic records from the early Oligocene (Fordyce, 2018; Marx and Uhen, 2010). During the Chattian flooding, cold climatic conditions prevailed, although there was a slight warming at the end, generating eustatic changes related to the opening of the Drake Passage and the origin of the Antarctic Circumpolar Current. During icehouse climate pulses, the tropical climate belt is compacted, which could allow faunal exchange between the North and South Pacific. The Gaarlandia intercontinental bridge may have closed the oceanic connection between the Atlantic and Pacific (Ali, 2012; Tong et al., 2018).

CONCLUSIONS

Cochimicetus convexus represents the first recorded Eomysticetidae fossil from the San Gregorio Formation and contributes significantly to the understanding of early mysticete evolution in the Northeast Pacific. Its basal position within Eomysticetidae, alongside *Echericetus novellus*, emphasizes Baja California Sur as a critical region for studying Oligocene cetacean diversity. Future work should focus on expanding the fossil record in the region, with particular attention to underexplored localities within the San Gregorio and El Cien formations. A broader collection of specimens will enhance our understanding of the morphological and biogeographical evolution of basal Chaeomysticeti.

ACKNOWLEDGMENTS

REFERENCES

Ali, J.R. 2012. Colonizing the Caribbean: is the GAARlandia land?bridge hypothesis gaining a foothold? Journal of Biogeography, 39(3):431–433.

Applegate, S.P. 1986. The El Cien Formation, strata of Oligocene and Early Miocene age in Baja California Sur. Revista Mexicana de Ciencias Geológicas, 6(2):145–162.

Barnes, L.G. 1998. The sequence of fossil marine mammal assemblages in Mexico. Avances en investigación: Paleontología de Vertebrados, Universidad Autónoma del Estado de Hidalgo. Publicación especial 1:26–79.

Barnes, L.G. 2002. Evolutionary history of the fossil marine mammals of Mexico, p. 125–226. In Montellano-Ballesteros, M. and Arroyo-Cabrales, J. (Coords.). Avances en los estudios paleomastozoológicos en México, Instituto Nacional de Antropología e Historia.

Barnes, L.G., Kimura, M., Furusawa, H., and Sawamura, H. 1994. Classification and distribution of Oligocene aetiocetidae (Mammalia; Cetacea; Mysticeti) from western North America and Japan. Island Arc, 3(4):392–431.

Bercovici, A., Hadley, A., and Villanueva-Amadoz, U. 2009. Improving depth of field resolution for palynological photomicrography. Palaeontologia Electronica, 12(2):1–12.
https://palaeo-electronica.org/2009_2/170/index.html

Berta, A., Lanzetti, A., Ekdale, E.G., and Deméré, T.A. 2016. From teeth to baleen and raptorial to bulk filter feeding in mysticete cetaceans: the role of paleontological, genetic, and geochemical data in feeding evolution and ecology. Integrative and Comparative Biology, 56(6):1271–1284.
https://doi.org/10.1093/icb/icw128

Bisconti, M. and Carnevale, G. 2022. Skeletal Transformations and the Origin of Baleen Whales (Mammalia, Cetacea, Mysticeti): A Study on Evolutionary Patterns. Diversity, 14(3):221.
https://doi.org/10.3390/d14030221

Bisconti, M., Pellegrino, L., and Carnevale, G. 2023. The chronology of mysticete diversification (Mammalia, Cetacea, Mysticeti): Body size, morphological evolution and global change. Earth Science Reviews, 239:104373.
https://doi.org/10.1016/j.earscirev.2023.104373

Boessenecker, R.W. and Fordyce, R.E. 2014. A new Eomysticetid (Mammalia: Cetacea) from the Late Oligocene of New Zealand and a re-evaluation of "Mauicetus" *waitakiensis*. Papers in Palaeontology, 1(2):107–140.
https://doi.org/10.31233/osf.io/4nqz2

Boessenecker, R.W. and Fordyce, R.E. 2015a. Anatomy, feeding ecology, and ontogeny of a transitional baleen whale: A new genus and species of Eomysticetidae (Mammalia: Cetacea) from the Oligocene of New Zealand. PeerJ, 3:e1129.
https://doi.org/10.7717/peerj.1129

Boessenecker, R.W. and Fordyce, R.E. 2015b. A new genus and species of eomysticetid (Cetacea: Mysticeti) and a reinterpretation of "Mauicetus" *lophocephalus* Marples, 1956: Transitional baleen whales from the upper Oligocene of New Zealand. Zoological Journal of the Linnean Society, 175(3):607–660.
https://doi.org/10.31233/osf.io/4nqz2

Boessenecker, R.W. and Fordyce, R.E. 2016. A new eomysticetid from the Oligocene Kokoamu Greensand of New Zealand and a review of the Eomysticetidae (Mammalia, Cetacea). Journal of Systematic Palaeontology, 15(6):429–469.
https://doi.org/10.1080/03036758.2016.1156552

Boessenecker, R.W. and Fordyce, R.E. 2017. Cosmopolitanism and Miocene survival of Eomysticetidae (Cetacea: Mysticeti) revealed by new fossils from New Zealand. New Zealand Journal of Geology and Geophysics. 60(2):145–157.
https://doi.org/10.1080/00288306.2017.1300176

Boessenecker, R.W., Beatty, B.L., and Geisler, J.H. 2023. New specimens and species of the Oligocene toothed baleen whale Coronodon from South Carolina and the origin of Neoceti. PeerJ, 11:e14795.
https://doi.org/10.7717/peerj.14795

Brisson, A.D. 1762. Regnum animale in classes IX Distributum, sive synopsis methodica. Theodorum Haak, Leiden.

Deméré, T.A. and Berta, A. 2008. Skull anatomy of the Oligocene toothed mysticete Aetioceus weltoni (Mammalia; Cetacea): implications for mysticete evolution and functional anatomy. Zoological Journal of the Linnean Society, 154(2):308–352.
https://doi.org/10.1111/j.1096-3642.2008.00414.x

de Muizon, C., Bianucci, G., Martínez-Cáceres, M., and Lambert, O. 2019. *Mystacodon selenensis*, the earliest known toothed mysticete (Cetacea, mammalia) from the late Eocene of Peru: Anatomy, phylogeny, and feeding adaptations. Geodiversitas, 41(11):401–499.
https://doi.org/10.5252/geodiversitas2019v41a11

Fischer, R., Galli-Oliver, C., Gidde, A., and Schwennicke, T. 1995. The El Cien Formation of Southern Baja California, México: Stratigraphic precisions. Newsletters on Stratigraphy, 32(1):137–161.

Flower, W.H. 1864. Notes on the skeletons of whales in the principal museums of Holland and Belgium, with descriptions of two species apparently new to science. Proceedings of the Zoological Society of London, 1864(1):382–420.

Fordyce, R.E. 2018. Cetacean Evolution, p. 180–195. In Wursig, B., Thewissen, J.G.M, and Kovacs, K.M. (eds.), Encyclopedia of Marine Mammals. Academic Press.

Fordyce, R.E. and Marx, F.G. 2018. Gigantism Precedes Filter Feeding in Baleen Whale Evolution. Current Biology, 28(10):1670–1676. https://doi.org/10.1016/j.cub.2018.04.027

Fordyce, R.E. and de Muizon, C. 2001. Evolutionary history of cetaceans: a review. Secondary adaptation of tetrapods to life in water, 169–233.

Föllmi, K.B., Schöllhorn, I., Ulianov, A., Adatte, T., Spangenberg, J.E., de Kaenel, E., and Garrison, R.E. 2019. Phosphogenesis during the Cenozoic transition from greenhouse to icehouse conditions: Upper Oligocene to lower Miocene siliceous, phosphate, and organic?rich sediments near La Purísima, Baja California Sur, Mexico. The Depositional Record, 5(1):23–52. https://doi.org/10.1002/dep2.52

Geisler, J.H., Boessenecker, R.W., Brown, M., and Beatty, B.L. 2017. The origin of filter feeding in whales. Current Biology, 27:2036–2042. https://doi.org/10.1016/j.cub.2017.06.003

Grimm, K.A. and Föellmi, K.B. 1994. Doomed pioneers: allochthonous crustacean tracemakers in anaerobic basinal strata, Oligo-Miocene San Gregorio Formation, Baja California Sur, Mexico. Palaios, 9(4):313–334. https://doi.org/10.2307/3515054

Goloboff, P.A., Farris, J.S., and Nixon, K.C. 2008. TNT, a free program for phylogenetic analysis. Cladistics, 24(5):774–786. https://doi.org/10.1111/j.1096-0031.2008.00217.x

Goloboff, P.A. and Morales, M.E. 2023. TNT version 1.6, with a graphical interface for MacOS and Linux, including new routines in parallel. Cladistics, 39(2):144–153. https://doi.org/10.1111/cla.12524

Hausback, B.P. 1984. Cenozoic volcanic and tectonic evolution of Baja California Sur, Mexico. Geology of the Baja California Peninsula: California, U.S.A. Pacific Section S.E.P.M., 39(1):219–236.

Hernández-Cisneros, A.E. 2018. A new group of late Oligocene mysticetes from México. Palaeontologia Electronica, 21(1):1–30. https://doi.org/10.26879/746

Hernández-Cisneros, A.E. and Nava Sánchez, E.N. 2022. Oligocene Dawn Baleen Whales in Mexico (Cetacea, Eomysticetidae) and Palaeobiogeographic Notes. Paleontología Mexicana, 11(1):1–12.

Hernández-Cisneros, A.E., Schwennicke, T., Rochín-Bañaga, H., and Tsai, C.H. 2024. *Echericetus novellus* n. gen. n. sp. (Cetacea, Mysticeti, Eomysticetidae), an Oligocene baleen whale from Baja California Sur, Mexico. Journal of Paleontology, 97(6):1309–1328. https://doi.org/10.1017/jpa.2023.80

Iturralde-Vinent, M. and MacPhee, R.D. 1999. Paleogeography of the Caribbean region: implications for Cenozoic biogeography. Bulletin of the AMNH, no. 238.

Kalinowski, S.T. 2009. How well do evolutionary trees describe genetic relationships between populations? Heredity, 102:506–513. https://doi.org/10.1038/hdy.2008.136

Kienle, S.S., Ekdale, E.G., Reidenberg, J.S., and Deméré, T.A. 2015. Tongue and hyoid musculature and functional morphology of a neonate gray whale (Cetacea, Mysticeti, Eschrichtius robustus). The Anatomical Record, 298(4):660–674. https://doi.org/10.1002/ar.23107

Lambert, O., Martínez-Cáceres, M., Bianucci, G., Di Celma, C., Salas-Gismondi, R., Steurbaut, E., and De Muizon, C. 2017. Earliest mysticete from the Late Eocene of Peru sheds new light on the origin of baleen whales. Current Biology, 27(10):1535–1541. https://doi.org/10.1016/j.cub.2017.04.026

Maddison, W.P. and Maddison, D.R. 2023. Mesquite: a modular system for evolutionary analysis. Version 3.81 http://www.mesquiteproject.org

Marx, F.G., Hocking, D.P., Park, T., Ziegler, T., Evans, A.R., and Fitzgerald, E.M. 2016a. Suction feeding preceded filtering in baleen whale evolution. Memoirs of Museum Victoria, 75(1):71–82.

Marx, F.G., Lambert, O., and Uhen, M.D. 2016b. Cetacean Paleobiology. John Wiley and Sons, Wiley-Blackwell.

Marx, F.G. and Uhen, M.D. 2010. Climate, critters, and cetaceans: Cenozoic drivers of the evolution of modern whales. Science, 327(5968):993–996.

Marx, F.G., Post, K., Bosselaers, M., and Munsterman, D.K. 2019. A large Late Miocene cetotheriid (Cetacea, Mysticeti) from the Netherlands clarifies the status of Tranatocetidae. PeerJ, 7:e6426.
https://doi.org/10.7717/peerj.6426

McLean, H. and Hausback, B.P. 1984. Reconnaissance geologic map of the La Purisima-Paso Hondo area, Baja California Sur, Mexico, 84-93.
https://doi.org/10.3133/ofr8493

McLean, H., Hausback, B.P., and Knapp, J.H. 1987. The Geology of West-Central Baja California Sur, Mexico. Bulletin United States Geological Survey, 1579:1–16.

Mead, J.G. and Fordyce, R.E. 2009. The therian skull: a lexicon with emphasis on the odontocetes. Smithsonian Contributions to Zoology, 627:1–248.

Mitchell, E.D. 1989. Vertebrate Paleontology Section. Canadian Journal of Fisheries and Aquatic Sciences, 46:2219–2235.

Okazaki, Y. 2012. A new mysticete from the upper Oligocene Ashiya Group, Kyushu, Japan and its significance to mysticete evolution. Bulletin of the Kitakyushu Museum of Natural History and Human History Series A (Natural History), 10(1):129–152.
https://doi.org/10.34522/kmnh.10.0_129

Omura, H. 1964. A systematic study of the hyoid bones in the baleen whales. Scientific Reports of the Whales Research Institute, 18:149–170.

Peredo, C.M. and Uhen, M.D. 2016. A new basal chaeomysticete (Mammalia: Cetacea) from the Late Oligocene Pysht Formation of Washington, USA. Papers in Palaeontology, 2(4):533–554.
https://doi.org/10.1002/spp2.1051

Peredo, C.M., Pyenson, N.D., and Boersma, A.T. 2017. Decoupling tooth loss from the evolution of baleen in whales. Frontiers in Marine Science, 4:67.

Peredo, C.M. and Pyenson, N.D. 2018. *Salishicetus meadi*, a new aetiocetid from the late Oligocene of Washington State, and implications for feeding transitions in early mysticete evolution. Royal Society Open Science, 5(4):172336.
https://doi.org/10.1098/rsos.172336

Peredo, C.M., Pyenson, N.D., Marshall, C.D., and Uhen, M.D. 2018. Tooth Loss Precedes the Origin of Baleen in Whales. Current Biology, 28(24):3992–4000.e2.
https://doi.org/10.1016/j.cub.2018.10.047

Sanders, A.E. and Barnes, L.G. 2002a. Paleontology of the Late Oligocene Ashley and Chandler Bridge Formations of South Carolina, 2: Mycromysticetus rothauseni, a primitive cetotheriid mysticete (Mammalia: Cetacea), p. 271–294. In Emry, R.J. (ed.), Cenozoic Mammals of Land and Sea: Tributes to the Career of Clayton E. Ray. Smithsonian Institution Press, Vol. 93.
https://doi.org/10.5479/si.00810266.93.179

Sanders, A.E. and Barnes, L.G. 2002b. Paleontology of the late Oligocene Ashley and Chandler Bridge formations of South Carolina, 3: Eomysticetidae, a new family of primitive mysticetes (Mammalia: Cetacea), p. 313–356. In Emry, R.J. (ed.), Cenozoic Mammals of Land and Sea: Tributes to the Career of Clayton E. Ray. Smithsonian Institution Press, Vol. 93.
https://doi.org/10.5479/si.00810266.93.179

Schwennicke, T. 1994. Deep and shallow water phosphorite bearing strata of the upper Oligocene of Baja California, Mexico San Juan member, El Cien Formation. Zentralblatt für Geologie und Paläontologie, 1:567–580.

Solis-Añorve, A., González-Barba, G., and Hernández-Rivera, R. 2019. Description of a new toothed mysticete from the Late Oligocene of San Juan de La Costa, BCS, México. Journal of South American Earth Sciences, 89:337–346.
https://doi.org/10.1016/j.jsames.2018.11.015

Solis-Añorve, A., González-Barba, G., Buono, R.M., Schwennicke, T., and Díaz-Cruz, J. 2022. Resultados preliminares de la descripción de un eomisticeto de la localidad "ten minute" del Oligoceno tardío (Formación El Cien), Baja California Sur, México. In Moreno Bedmar, J.A. (Ed.), Memorias del Congreso número 6: XVII Congreso Nacional de Paleontología, Hermosillo, Sonora, México. Sociedad Mexicana de Paleontología A.C. and Instituto de Geología, UNAM, 85.

Solis-Añorve, A., González-Barba, G., Buono, M.R., Schwennicke, T., and Díaz-Cruz, J.A. 2024. The first record of an Eomysticetidae from the El Cien Formation (late Oligocene), "Ten Minute" locality, Baja California Sur, Mexico. Boletín de la Sociedad Geológica Mexicana, 76(1):A131223.76.
https://doi.org/10.18268/BSGM2024v76n1a131223

Tanaka, Y. 2024. A feeding organ the basihyal and thyrohyal tells which size of prey do true baleen whales (Cetacea, Chaeomysticeti) eat. Palaeontologia Electronica, 27(1):1–22.
https://doi.org/10.26879/1311

Tong, Y., Binford, G., Rheims, C.A., Kuntner, M., Liu, J., and Agnarsson, I. 2018. Huntsmen of the Caribbean: Multiple tests of the GAARlandia hypothesis. Molecular Pylogenetics and Evolution, 130:259–268.

Tsai, C.H. 2023. In search of the origin of crown Mysticeti. Journal of the Royal Society of New Zealand,
https://doi.org/10.1080/03036758.2023.2249410

Tsai, C.H. and Ando, T. 2015. Niche partitioning in Oligocene toothed mysticetes (Mysticeti: Aetiocetidae). Journal of Mammal Evolution, 23:33.
https://doi.org/10.1007/s10914-015-9292-y

Tsai, C.H. and Fordyce, R.E. 2015. The earliest gulp-feeding mysticete (Cetacea: Mysticeti) from the Oligocene of New Zealand. Journal of Mammal Evolution, 22:355.
https://doi.org/10.1007/s10914-015-9290-0

Tsai, C.H. and Fordyce, R.E. 2016. Archaic baleen whale from the Kokoamu Greensand: earbones distinguish a new late Oligocene mysticete (Cetacea: Mysticeti) from New Zealand. Journal of the Royal Society of New Zealand, 46:1–22.
https://doi.org/10.1080/03036758.2016.1156552

Tsai, C.H. and Fordyce, R.E. 2018. A new archaic baleen whale *Toipahautea waitaki* (early Late Oligocene, New Zealand) and the origins of crown Mysticeti. Royal Society Open Science, 5(4):172453.
https://doi.org/10.1098/rsos.172453

Uhen, M.D. 2008. New protocetid whales from Alabama and Mississippi, and a new cetacean clade, Pelagiceti. Journal of Vertebrate Paleontology, 28(3):589–593.
https://doi.org/10.1671/0272-4634(2008)28[589:NPWFAA]2.0.CO;2

Uhen, M.D. and Pyenson, N.D. 2007. Diversity estimates, biases, and historiographic effects: resolving cetacean diversity in the Tertiary. Palaeontologia Electronica, 10.2.11A:22.
http://palaeo-electronica.org/2007_2/00123/index.html

Werth, A.J. 2007. Adaptations of the cetacean hyolingual apparatus for aquatic feeding and thermoregulation. The Anatomical Record: Advances in Integrative Anatomy and Evolutionary Biology: Advances in Integrative Anatomy and Evolutionary Biology, 290(6): 546–568.

Westerhold, T., Marwan, N., Drury, A.J., Liebrand, D., Agnini, C., Anagnostou, E., and Zachos, J.C. 2020. An astronomically dated record of Earth's climate and its predictability over the last 66 million years. Science, 369(6509):1383–1387.

Zachos, J., Pagani, M., Sloan, L., Thomas, E., and Billups, K. 2001. Trends, rhythms, and aberrations in global climate 65 Ma to present. Science, 292(5517):686–693.
https://doi.org/10.1126/science.1059412

APPENDIX.

FIGURE S1. Photography of the ventral view with emphasis on the posterior region of the left mandible of *Cochimicetus convexus*. Scale bar 5 cm.

FIGURE S2. Photography of the dorsal-lateral view with emphasis on the coronoid process of the left mandible. Scale bar 5 cm.

FIGURE S3. Photography of the posterior lateral view emphasizing the zygomatic process in the image. Scale bar 5 cm.
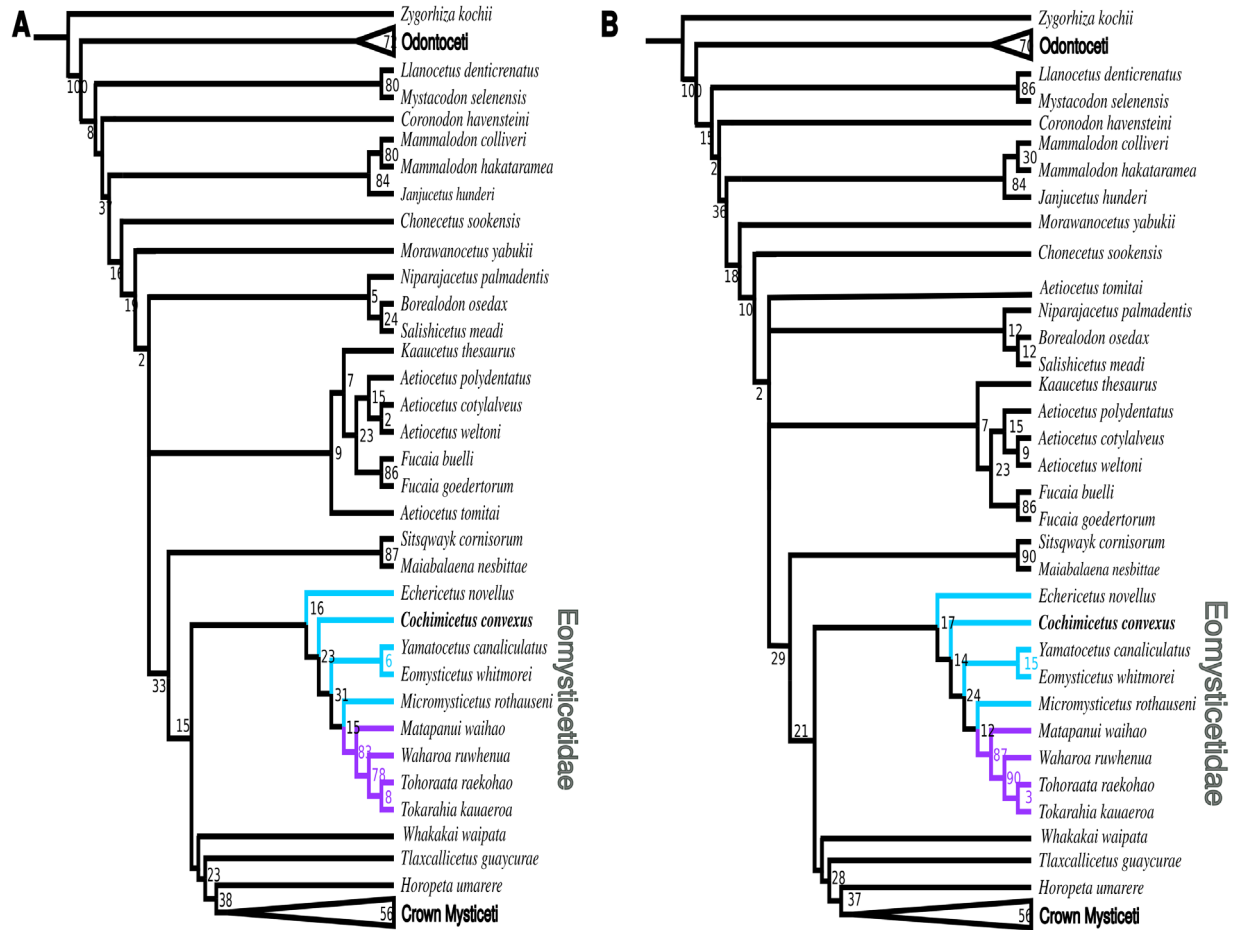
FIGURE S4. A, Implied weights with K 6; CI 0.259; RI 0.745; 89.35148 total length. **B**, Implied weights with K 12; CI 0.261; RI: 0.747; 57.74474 total length.